Int. J. Math. And Appl., 8(2)(2020), 87–97
ISSN: 2347-1557
Available Online: http://ijmaa.in/

International Journal of *Mathematics And its Applications*

Amazing Effects of Second Order Chemical Reaction, Radiation, and Soret-Dufour on MHD Flow of Walter's B Viscoelastic Fluid Past a Vertical Porous Plate

A. K. Shukla[1,*], Rajmani Yadav[2] and Santosh Kumar Chauhan[1]

1 Department of Mathematics, RSKD PG College, Jaunpur, India.

2 Department of Mathematics, Sant Gani Nath Government PG College, Mohammadabad Gohna Mau, India.

Abstract: The focus of this paper is to study magnetohydrodynamics Walter's B viscoelastic fluid flow over a vertical porous plate embedded in a porous medium under the influence of the Soret-Dufour effect, radiation effect, and second order chemical reaction. The contemplated fact is modeled by a system of nonlinear partial differential equations influenced by the boundary conditions. The governing coupled nondimensional partial differential equations solved numerically using Crank-Nicolson implicit finite difference method. Under the influence of governing flow parameters, results for velocity, temperature, and concentration are computed and portrayed through graphs while the numerical values for skin friction, Nusselt number, and Sherwood number are presented with the help of tables.

MSC: 76W05, 80A20, 80A21, 80A32, 80M20

Keywords: Chemical reaction, Magnetohydrodynamics, Walter's B model, Heat and Mass transfer, Soret and Dufour effects, radiation effect, Crank-Nicolson finite difference method.

1. Introduction

Viscoelastic fluids are generally seen in things such as clay coating, fiber technology, exotic lubricants and variety of foodstuff, etc. For the last many years, many research workers have been attracted towards the investigation of Soret and Dufour effect on MHD viscoelastic fluid flow problems because of engineering and manufacturing applications such as glass fiber production, polymer extrusion, and ethylene glycol mixture, etc. For the accurate simulation of viscoelastic fluid, Walter's B model has been applied.

Taleghani and Heydari [1] investigated heat transfer in non-Newtonian MHD viscoelastic fluid flow expanded on a horizontal plane. Gizachew and Shankar studied the Non-Newtonian MHD flow of viscoelastic fluid on a stretching sheet under the influence of viscous dissipation and heat generation/absorption. G. Subba Reddy et al. [4] explained the effect of radiation and Hall current on an unsteady MHD free convective flow in a vertical plate immersed in a porous medium. K. V. B. Rajakumar et al. [6] explored the effects of Dufour, chemical reaction, Hall, ion slip current, and thermal radiation on unsteady MHD viscoelastic fluid flow past an impulsively started infinite vertical plate embedded in a porous medium. Dulal et al. [8] studied Soret–Dufour effects on MHD flow over an inclined plate in presence of heat source/sink and chemical reaction.

* *E-mail: ashishshukla1987@gmail.com*

Hussain et al. [3] has given contribution in the study of the bi-phase couple stress nanofluid over an inclined plate having Hafnium particles and partially submerged metallic particles. Hoseini et al. [5] studied the influence of radiation, free convection, Joule heating on the heat transfer rates of Walters's B viscoelastic nanofluid flow past an inclined stretching plate. Idrees et al. [7] investigated impact entropy generation for the various molecular liquids in an MHD nanofluid in a rotating channel. Rahila Naz et al. [9] studied the impact of Joule heating, inclined magnetic field, viscous dissipation, swimming microorganisms in Walter's B nanofluid stratification flowing past a horizontal cylindrical surface.

Akram et al. [10] analyzed using a variational iteration method study of MHD flow in a porous medium. Jabeen et al. [11] has given Analysis of the MHD Flow over a curved Stretching Sheet in a Porous Medium. Idowu and Falodun [12] studied non-Newtonian fluids flow through a vertical porous plate under the influence of Soret-Dufour, thermal conductivity and viscosity using the spectral homotopy analysis method.

This paper aims to study the influence of second-order chemical reaction, Soret-Dufour effect, radiation on MHD Walter's B viscoelastic fluid flow past a vertical porous plate embedded in a porous medium with variable temperature and concentration. The governing nonlinear partial differential equations of flow regime are solved with the help of Crank-Nicolson implicit finite difference method. On account of the variation of physical parameters velocity, temperature, and concentration profiles are discussed with the help of graphs. Different values for various physical parameters Skin friction coefficient, Nusselt number, and Sherwood number are given in tables.

2. Mathematical Model of Flow Problem

Consider an unsteady MHD viscoelastic fluid flow over a vertical porous plate embedded in a porous medium under the influence of second order chemical reaction, radiation, and Soret-Dufour effect. Soret-Dufour effects are significant because of the level of species concentration is assumed to be large. The temperature and concentration of the fluid of the plate surface are $\tilde{\Theta}_p$ and $\tilde{\Phi}_p$ respectively. Also, the free-stream temperature and concentration of the fluid are represented by $\tilde{\Theta}_\infty$ and $\tilde{\Phi}_\infty$ respectively. The applied magnetic field with uniform strength B_0 acts in the perpendicular direction to the flow. $\tilde{x}$-axis and $\tilde{y}$-axis is taken along and normal to plate respectively. The flow variables are functions of $\tilde{y}$ and $\tilde{t}$ only because of infinite length in $\tilde{x}$ direction. Considering the above assumptions, the governing equations of the flow regime are given by:

$$\frac{\partial \tilde{v}}{\partial \tilde{y}} = 0 \Rightarrow \tilde{v} = -v_0 \text{ (fixed)} \tag{1}$$

$$\frac{\partial \tilde{u}}{\partial \tilde{y}} + \tilde{v}\frac{\partial \tilde{u}}{\partial \tilde{y}} = \nu \frac{\partial^2 \tilde{u}}{\partial \tilde{y}^2} - \tilde{\lambda}\frac{\partial^3 \tilde{u}}{\partial \tilde{y}^2 \partial \tilde{t}} + g\beta_t(\tilde{\Theta} - \tilde{\Theta}_\infty) + g\beta_c(\tilde{\Phi} - \tilde{\Phi}_\infty) - \frac{\sigma B_0^2 \tilde{u}}{\rho} - \frac{\nu \tilde{u}}{\tilde{K}} \tag{2}$$

$$\rho c_p \left(\frac{\partial \tilde{\Theta}}{\partial \tilde{t}} + \tilde{v}\frac{\partial \tilde{\Theta}}{\partial \tilde{y}}\right) = k\frac{\partial^2 \tilde{\Theta}}{\partial \tilde{y}^2} - \frac{\partial a_r}{\partial \tilde{y}} + \frac{\rho D_m k_\Theta}{c_s}\frac{\partial^2 \tilde{\Phi}}{\partial \tilde{y}^2} \tag{3}$$

$$\frac{\partial \tilde{\Phi}}{\partial \tilde{t}} + \tilde{v}\frac{\partial \tilde{\Phi}}{\partial \tilde{y}} = D_m \frac{\partial^2 \tilde{\Phi}}{\partial \tilde{y}^2} + \frac{D_m k_\Theta}{\Theta_m}\frac{\partial^2 \tilde{\Theta}}{\partial \tilde{y}^2} - \tilde{Ch}(\tilde{\Phi} - \tilde{\Phi}_\infty)^2 \tag{4}$$

boundary conditions for this governing fluid flow model are

$$\begin{aligned}
&\tilde{t} \le 0 \quad \tilde{u} = 0 \quad \tilde{\Theta} = \tilde{\Theta}_\infty \quad \tilde{\Phi} = \tilde{\Phi}_\infty \quad \forall\, \tilde{y} \\
&\tilde{t} > 0 \quad \tilde{u} = U_0 \quad \tilde{\Theta} = \tilde{\Theta}_\infty + (\tilde{\Theta}_p - \tilde{\Theta}_\infty)e^{-\tilde{N}\tilde{t}}, \\
&\tilde{\Phi} = \tilde{\Phi}_\infty + (\tilde{\Phi}_p - \tilde{\Phi}_\infty)e^{-\tilde{N}\tilde{t}}, \quad at\ \tilde{y} = 0 \\
&\tilde{u} = 0 \quad \tilde{\Theta} \to \tilde{\Theta}_\infty \quad \tilde{\Phi} \to \tilde{\Phi}_\infty \quad \tilde{y} \to \infty
\end{aligned} \tag{5}$$

where $\tilde{N} = \frac{v_0^2}{\nu}$, $\tilde{\Theta}$ and $\tilde{\Phi}$ are temperature and concentration of flow regime, $\tilde{\Theta}_\infty$ and $\tilde{\Phi}_\infty$ are temperature and concentrationof free stream, due to second order chemical reaction this term $\tilde{Ch}(\tilde{\Phi} - \tilde{\Phi}_\infty)^2$ has introduced, $\tilde{Ch}$ is chemical reaction constant,

β_t is volumetric coefficient of thermal expansion, β_c is coefficient of volume expansion, a_r is radiation coefficient, ν is kinematic viscosity and Θ_m is mean fluid temperature, $\tilde{v}$ is suction velocity, $\tilde{\lambda}$ is Walter's-B viscoelasticity parameter, $\tilde{K}$ is permeability of porous medium, σ is electrical conductivity, D_m is molecular diffusivity, g is acceleration due to gravity, k_Θ is thermal diffusion ratio, μ is viscosity, ρ is fluid density, k is thermal conductivity of fluid, c_p is specific heat at constant pressure.

The radiative flux a_r with the help of Rosseland approximation[14], is given by

$$a_r = -\frac{4\tilde{\sigma}}{3c_m}\frac{\partial \tilde{\Theta}^4}{\partial \tilde{y}} \tag{6}$$

where c_m is mean Rosseland radiative absorption constant and $\tilde{\sigma}$ is Stefan Boltzmann constant. In this model, $\tilde{\Theta}^4$ may be resolved as linearly in terms of temperature because of the temperature difference within a flow regime is very low. It is made up by expanding $\tilde{\Theta}^4$ in a Taylor series about $\tilde{\Theta}_\infty$, as prosecute

$$\tilde{\Theta}^4 = \tilde{\Theta}_\infty^4 + (\tilde{\Theta} - \tilde{\Theta}_\infty)3\tilde{\Theta}_\infty^3 + \frac{(\tilde{\Theta} - \tilde{\Theta}_\infty)^2}{2!}12\tilde{\Theta}_\infty^2 + \cdots \tag{7}$$

neglecting higher-order terms of Θ_∞ in above expansion, we get

$$\tilde{\Theta}^4 \cong 4\tilde{\Theta}_\infty^3\tilde{\Theta} - 3\tilde{\Theta}_\infty^4 \tag{8}$$

hence, with the help of equations 6 and 8, equation 3 is rewritten as

$$\rho c_p\left(\frac{\partial \tilde{\Theta}}{\partial \tilde{t}} + \tilde{v}\frac{\partial \tilde{\Theta}}{\partial \tilde{y}}\right) = k\frac{\partial^2 \tilde{\Theta}}{\partial \tilde{y}^2} + \frac{16\tilde{\sigma}\tilde{\Theta}_\infty^3}{3c_m}\frac{\partial^2 \tilde{\Theta}}{\partial \tilde{y}^2} + \frac{\rho D_m k_\Theta}{c_s}\frac{\partial^2 \tilde{\Phi}}{\partial \tilde{y}^2} \tag{9}$$

To achieve dimensionless governing partial differential equations, we deputized the following dimensionless quantities

$$\begin{aligned}
&\lambda = \frac{\lambda_0 v_0^2}{\nu^2},\ So = \frac{D_m k_\Theta(\tilde{\Theta}_p - \tilde{\Theta}_\infty)}{\Theta_m \nu(\tilde{\Phi}_p - \tilde{\Phi}_\infty)},\ R = \frac{4\tilde{\sigma}\tilde{\Theta}_\infty^3}{c_m k},\ Sc = \frac{\nu}{D_m},\ K = \frac{v_0^2\tilde{K}}{\nu^2},\ Pr = \frac{\mu c_p}{k},\\
&u = \frac{\tilde{u}}{U_0},\ t = \frac{\tilde{t}v_0^2}{\nu},\ \theta = \frac{\tilde{\Theta} - \tilde{\Theta}_\infty}{\tilde{\Theta}_p - \tilde{\Theta}_\infty},\ \Phi = \frac{\tilde{\Phi} - \tilde{\Phi}_\infty}{\tilde{\Phi}_p - \tilde{\Phi}_\infty},\ Gm = \frac{\nu g\beta_c(\tilde{\Phi}_p - \tilde{\Phi}_\infty)}{U_0 v_0^2},\\
&Gr = \frac{\nu g\beta_t(\tilde{\Theta}_p - \tilde{\Theta}_\infty)}{U_0 v_0^2},\ y = \frac{\tilde{y}v_0}{\nu},\ Ch = \frac{\tilde{C}h\nu}{v_0^2},\ Df = \frac{D_m k_\Theta(\tilde{\Phi}_p - \tilde{\Phi}_\infty)}{c_s c_p \nu(\tilde{\Theta}_p - \tilde{\Theta}_\infty)},\ M = \frac{\sigma B_0^2\nu}{\rho v_0^2}
\end{aligned} \tag{10}$$

.

where λ, Pr, K, M, So, Gm, Gr, R, Sc, Df and Ch are respectively viscoelastic parameter, Prandtl number, permeability parameter, magnetic parameter, Soret number, solutal Grashof number, thermal Grashof number, radiation parameter, Schmidt number, Dufour number and chemical reaction parameter.

Applying these non dimensional quantities in equations 2, 9 and 4, we found dimensionless form of governing non linear partial differential equations as follows:

$$\frac{\partial u}{\partial t} - \frac{\partial u}{\partial y} = \frac{\partial^2 u}{\partial y^2} - \lambda\frac{\partial^2 u}{\partial y^2 \partial t} + Gr\,\theta + Gm\,\Phi - M\,u + \frac{u}{K} \tag{11}$$

$$\frac{\partial \theta}{\partial t} - \frac{\partial \theta}{\partial y} = \frac{1}{Pr}\left(1 + \frac{4R}{3}\right)\frac{\partial^2 \theta}{\partial y^2} + Du\frac{\partial^2 C}{\partial y^2} \tag{12}$$

$$\frac{\partial \Phi}{\partial t} - \frac{\partial \Phi}{\partial y} = \frac{1}{Sc}\frac{\partial^2 \Phi}{\partial y^2} + Sr\frac{\partial^2 \theta}{\partial y^2} - Ch\,\Phi^2 \tag{13}$$

with boundary conditions:

$$\begin{aligned} &t \leq 0 \quad u = 0, \quad \theta = 0, \quad \Phi = 0, \quad \forall\, y \\ &t > 0 \quad u = 1, \quad \theta = e^{-t}, \quad \Phi = e^{-t}, \quad at\ y = 0 \\ &u = 0, \quad \theta \to 0, \quad \Phi \to 0, \quad y \to \infty. \end{aligned} \tag{14}$$

Many mathematical analyst have an interest in examined changes in physical quantities like skin-friction coefficients S_f along with the plate, Nusselt number N_Θ, and Sherwood number S_Φ. This is given by which is written in dimensionless form as

$$\begin{aligned} S_f &= \left(\frac{\partial u}{\partial y}\right)_{y=0} \\ N_\Theta &= -\left(\frac{\partial \theta}{\partial y}\right)_{y=0} \\ S_\Phi &= -\left(\frac{\partial \Phi}{\partial y}\right)_{y=0} \end{aligned} \tag{15}$$

3. Method of Solution

Additional difficulties in the analytical solution part have led us to apply a numerical method. In order to get a solution of the flow model for the above system of partial differential equations 11, 12 and 13 under influence of the boundary conditions 13 for multiple values of the governing physical parameters, Crank-Nicolson implicit finite difference method have been employed to investigate. After employing this method, the transformed system of partial differential equations come in form:

$$\begin{aligned} \frac{u_{q,w+1} - u_{q,w}}{\Delta t} - \frac{u_{q+1,w} - u_{q,w}}{\Delta y} =& \left(\frac{u_{q-1,w} - 2u_{q,w} + u_{q-1,w} - 2u_{q,w+1} + u_{q+1,w+1}}{2(\Delta y)^2}\right) \\ &- \lambda\left(\frac{u_{q-1,w} - 2u_{q,w} + u_{q-1,w} - 2u_{q,w+1} + u_{q+1,w+1}}{2(\Delta y)^2 \Delta t}\right) + Gr\left(\frac{\theta_{q,w+1} - \theta_{q,w}}{2}\right) \\ &+ Gm\left(\frac{\Phi_{q,w+1} - \Phi_{q,w}}{2}\right) - \left(M + \frac{1}{K}\right)\left(\frac{u_{q,w+1} + u_{q,w}}{2}\right) \end{aligned} \tag{16}$$

$$\begin{aligned} \frac{\theta_{q,w+1} - \theta_{q,w}}{\Delta t} - \frac{\theta_{q+1,w} - \theta_{q,w}}{\Delta y} =& \frac{1}{Pr}\left(1 + \frac{4R}{3}\right)\left(\frac{\theta_{q-1,w} - 2\theta_{q,w} + \theta_{q-1,w} - 2\theta_{q,w+1} + \theta_{q+1,w+1}}{2(\Delta y)^2}\right) \\ &+ Df\left(\frac{\Phi_{q-1,w} - 2\Phi_{q,w} + \Phi_{q-1,w} - 2\Phi_{q,w+1} + \Phi_{q+1,w+1}}{2(\Delta y)^2}\right) \end{aligned} \tag{17}$$

$$\begin{aligned} \frac{\Phi_{q,w+1} - \Phi_{q,w}}{\Delta t} - \frac{\Phi_{q+1,w} - \Phi_{q,w}}{\Delta y} =& \frac{1}{Sc}\left(\frac{\Phi_{q-1,w} - 2\Phi_{q,w} + \Phi_{q-1,w} - 2\Phi_{q,w+1} + \Phi_{q+1,w+1}}{2(\Delta y)^2}\right) \\ &+ So\left(\frac{\theta_{q-1,w} - 2\theta_{q,w} + \theta_{q-1,w} - 2\theta_{q,w+1} + \theta_{q+1,w+1}}{2(\Delta y)^2}\right) - Ch\left(\frac{\Phi_{q,w+1} + \Phi_{q,w}}{2}\right)^2 \end{aligned} \tag{18}$$

boundary conditions are also written as:

$$\begin{aligned} &u_{q,0} = 0 \quad \theta_{q,0} = 0 \quad \Phi_{q,0} = 0 \quad \forall\, q \\ &u_{0,w} = 1 \quad \theta_{0,w} = e^{-w\Delta t} \quad \Phi_{0,w} = e^{-w\Delta t} \\ &u_{n,w} = 0 \quad \theta_{n,w} \to 0 \quad \Phi_{n,w} \to 0 \end{aligned} \tag{19}$$

where q signifies division of y-axis, $\Delta y = y_{q+1} - y_q$ and w signifies to division of time t, $\Delta t = t_{w+1} - t_w$.So our aim is to calculate the values of u, θ and Φ at time t, for this calculate the values at time $t + \Delta t$ as follows: first we employ $q = 1, 2, ..., n-1$, n represents to ∞ thus equations 16 to 18 give us tridiagonal system of non linear equations together boundary conditions in equation 19, are solved by using Thomos algorithm phenomena as given in Luther et al.[13], get the values of θ and Φ $\forall$ y at $t + \Delta t$. Equation 16 is solved for u till desired time t using this to replace these values of θ and Φ.

4. Results and Discussion

The calculation is completed for multiple sets of values of the governing physical parameters namely, Prandtl number Pr, the magnetic parameter M, Soret number So, Dufour number Df, Chemical reaction parameter Ch, the Schmidt number Sc, thermal Grashof number Gr, the solutal Grashof number Gm, permeability parameter K, and viscoelastic parameter λ. Stand for getting clean permeance into the physical problem, numerical results are shown with the help of graphs. Graphical demonstration of the results is more helpful and able to a practical discussion of the influence of various parameters. To reaffirm these results, the numerical calculation of skin friction coefficients S_f, Nusselt number N_Θ, and Sherwood number S_Φ are displayed in a tabular view.

Figures 1, 3 and 2 show the influence of chemical reaction parameter Ch on velocity, temperature and concentration profiles, respectively.The velocity and concentration profiles are reduced utilizing increment in chemical reaction parameter, while the discord effect exist in the case of temperature. The contribution of Schmidt number is ilustrated in figure 4. It is noticed that velocity decrease rapidly in starting after that decrement is slow as Schmidt number varies as well as it is also seen that change in concentration profiles in figure 6 same as change in velocity profiles, on the other hand in figure 5 temperature profile increases when Schmidt number increases. Figures 7, 8 and 9 are depicted that the variation of radiation parameter R on the velocity u, temperature θ and concentration Φ . It is analysed that a change in the radiation parameter results in increasing velocity and temperature while there is two type of changes seen in concentration like it decreases near to plate after then it increases, it is very interesting result and circled in figure.

In figures 10 and 11, it is analysed that velocity profiles and temperature profiles decrease whereas an increase in Prandtl number Pr. Now those for concentration in figure 12, interesting result has come and circled that first near to plate concentration profile increases hereafter it decreases. Figures 13, 14 and 15 elucidate the variation of Dufour parameter Df on the velocity u, temperature θ and concentration Φ fields. It is seen that an increase in the values of Df increases the velocity, temperature profiles in boundary layer. An increment in values of Df is noteworthy change in concentration that near to wall it decreases thereafter it increases. Good change in velocity profiles in figure 16 has been seen that increase in magnetic parameter M result as velocity decreases.

Figures 17, 18 and 19 delineate the effect of Soret number So on the velocity, temperature and concentration profiles receptively. Increment in Soret number So is indicate velocity profiles and boundary layer thickness increase. Increase in values of Soret number So, temperature profiles decreases near to plate and thereafter increases in figure 18 as well as thermal boundary layer thickness increase. Concentration profiles and boundary layer thickness increases when Soret number So increases in figure 19.

Boundary layer thickness of momentum, thermal and species transfer in figures 20, 21 and 22 respectively are shown as time t changes. Figure 23 depicts change of viscoelstic parameter λ that near to plate ther is no change in velocity profiles thereafter increases after then again there is no change in velocity. It is also noticed that there is no change in boundary layer thickness. The values of the skin friction coefficient S_f, Nusslet number N_Θ, and Sherwood number S_Φ for multiple values of governing physical parameters in table 1.From table it is clear that on increase Dufour number Df, Soret number So, Radiation parameter R, variation in time t skin friction coefficient S_f increases whereas on increasing Schmidt number Sc, viscoelastic parameter λ, Prandtl number Pr, magnetic parameter M and chemical reaction parameter Ch, S_f decreases. Nusslet number N_Θ decreases and Sherwood number S_Φ increases as Dufour number, Chemical reaction parameter, Schmidt number, radiation parameter, variation in time. On the other hand Nusselt number N_Θ increases and Sherwood number S_Φ decreases as Soret number and Prandtl number increase.

5. Conclusion

In this analysis, a numerical solution of unsteady MHD free convective heat and mass transfer flow of incompressible, electrically conducting Walter's B viscoelastic fluid over vertical porous plate embedded in a porous medium in the presence of second order chemical reaction, radiation, and Soret-Dufour effects has been investigated. The observation of this study are as follows

1. Radiation parameter has the effect of decreasing momentum boundary layer thickness.
2. Boundary layer thickness of species transfer increases as the Soret number increases as well as there is an interesting change in concentration near the plate.
3. Dufour number increases then concentration decreases near to plate and after mid of boundary layer thickness concentration increases slowly
4. There is an amazing change in velocity and concentration for different values of Schmidt number that both decrease very fast first and then the rate of decrement is slow.

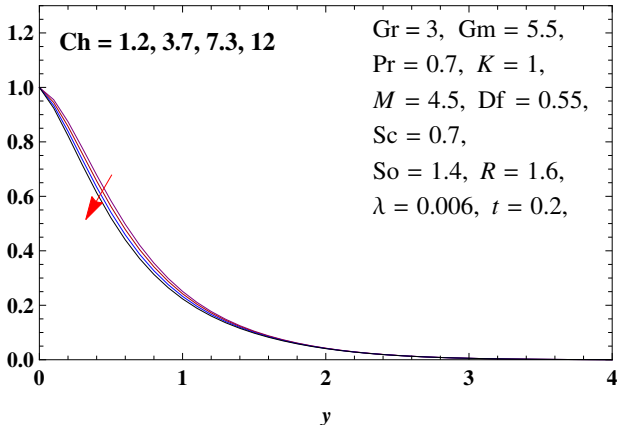

Figure 1. **Change in velocity for multiple values of Ch**

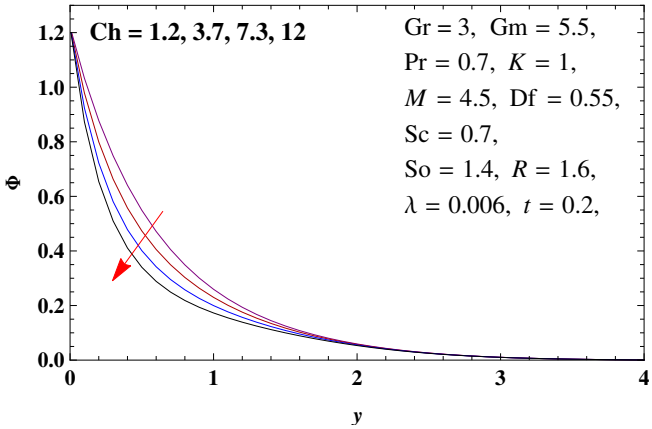

Figure 2. Change in Concentration for multiple Values of Ch

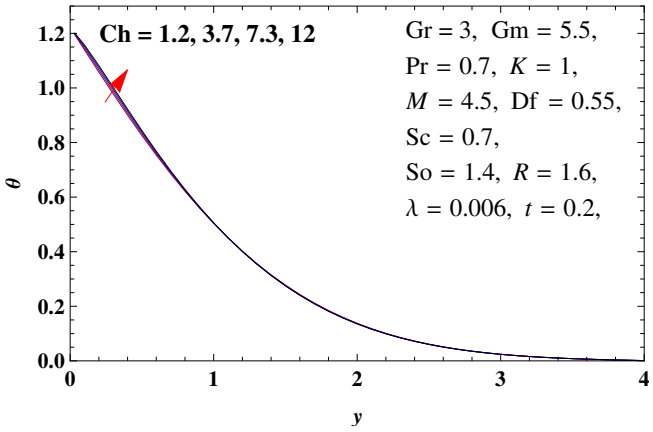

Figure 3. Change in temperature for various values of Ch

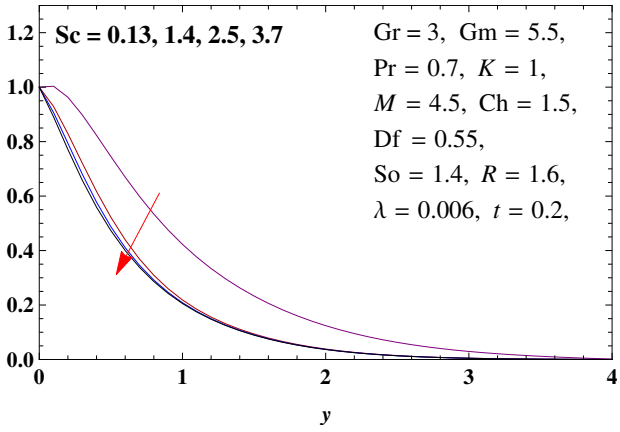

Figure 4. **Change in velocity for multiple values of Sc**

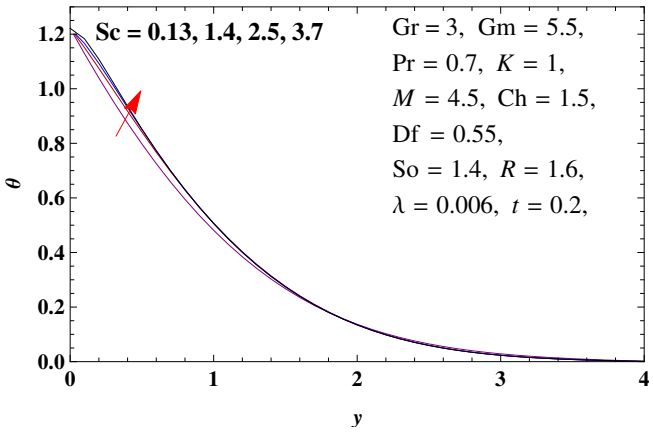

Figure 5. change in temperature for different values of Sc

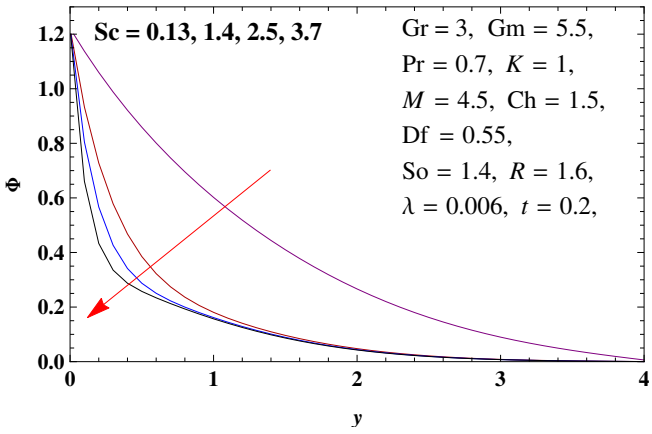

Figure 6. Change in concentration for various values of Sc

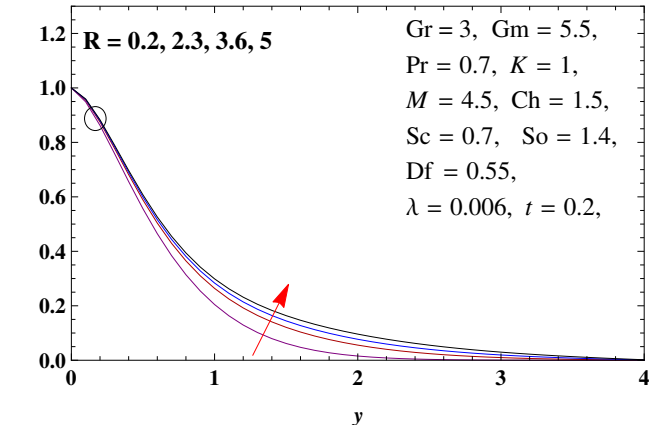

Figure 7. **Change in velocity for multiple values of R**

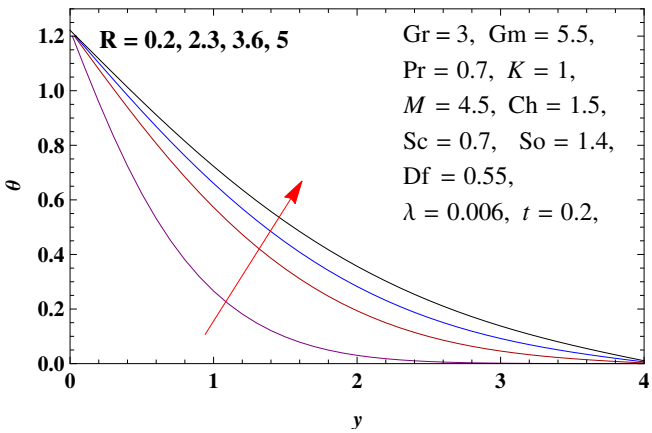

Figure 8. Change in temperature for different values of R

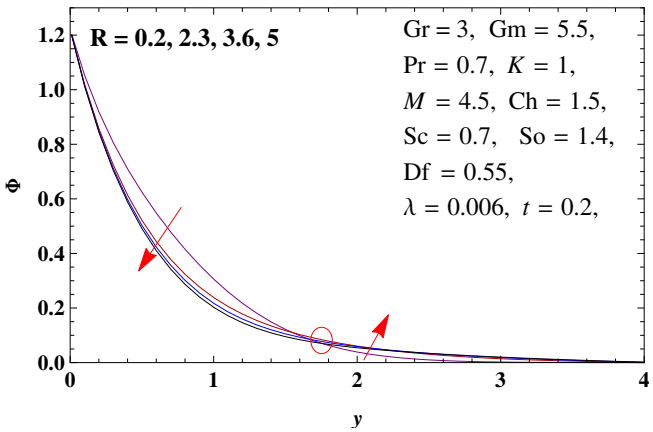

Figure 9. **Change in concentration for various values of R**

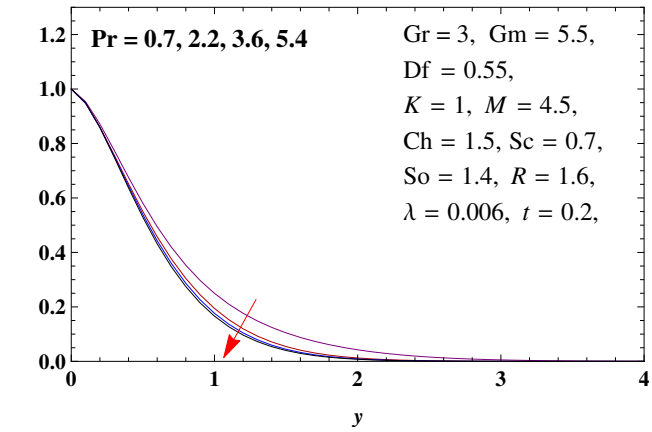

Figure 10. **Change in velocity for multiple values of Pr**

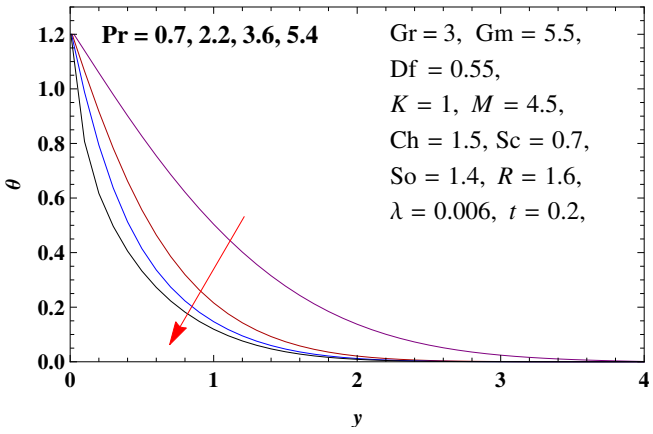

Figure 11. Change in temperature for multiple values of Pr

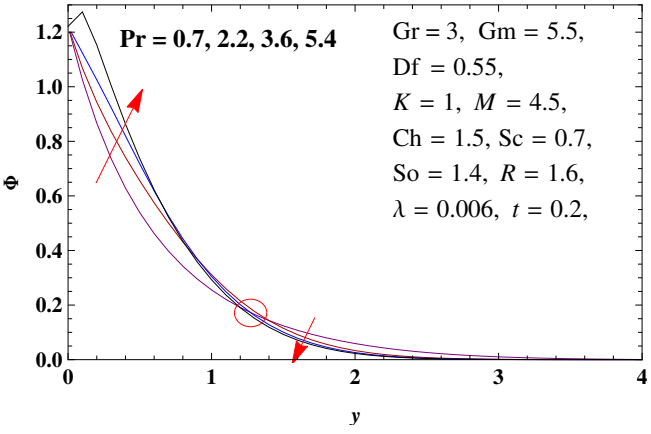

Figure 12. **Change in velocity for different values of Pr**

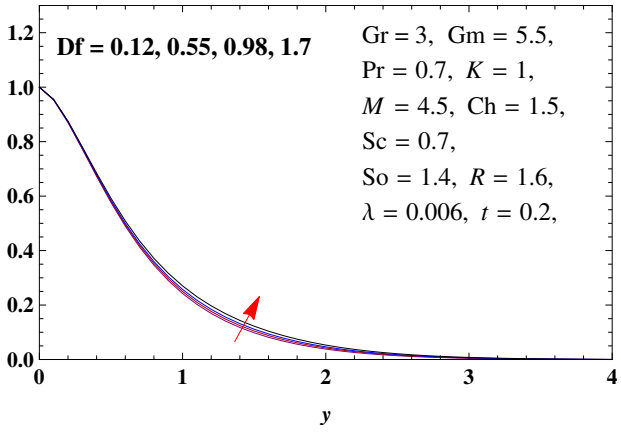

Figure 13. **Change in velocity for different values of Df**

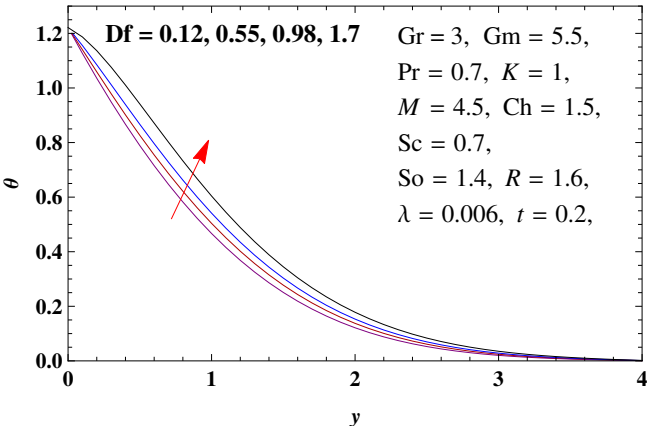

Figure 14. Change in temperature for multiple values of Df

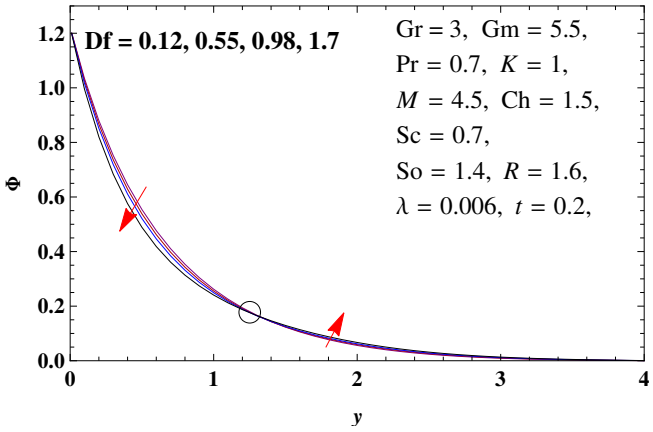

Figure 15. Change in concentration for various values of Df

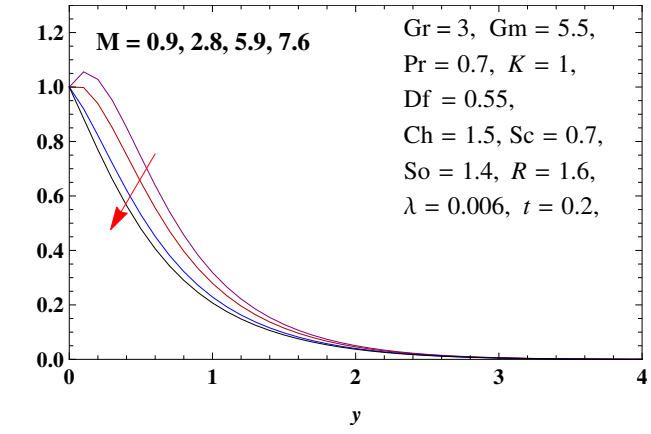

Figure 16. **Change in velocity for multiple values of M**

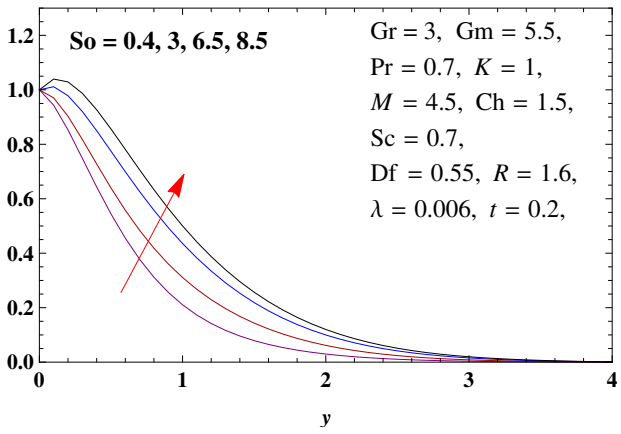

Figure 17. **Change in velocity for multiple values of Sr**

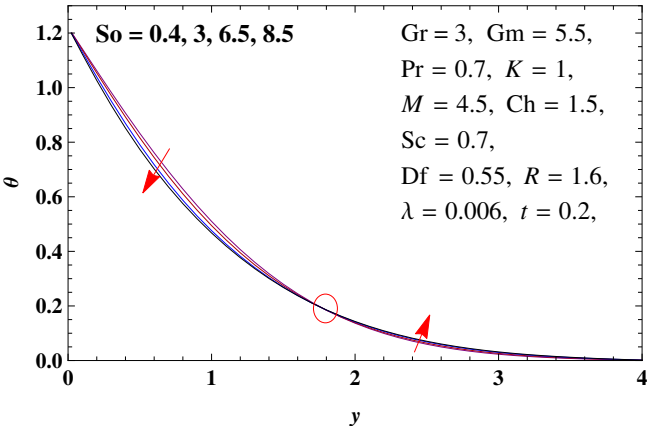

Figure 18. Change in temperature for multiple values of Sr

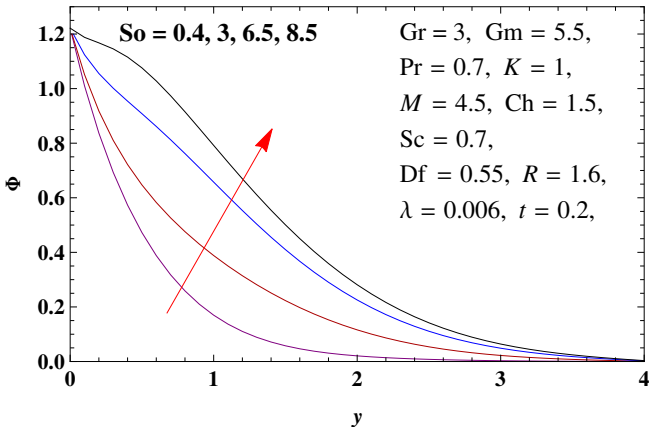

Figure 19. Change in concentration for different values of Sr

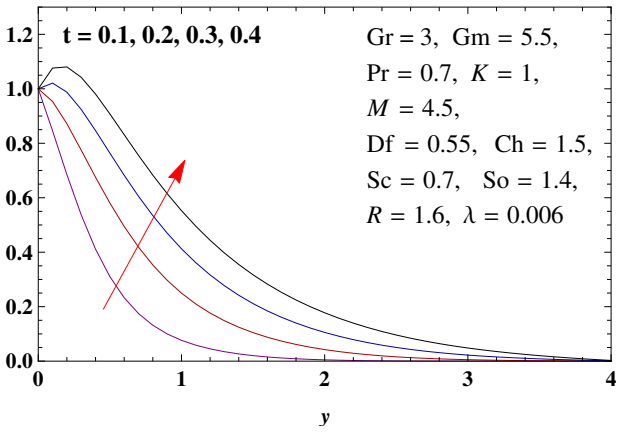

Figure 20. **Change in velocity for multiple values of t**

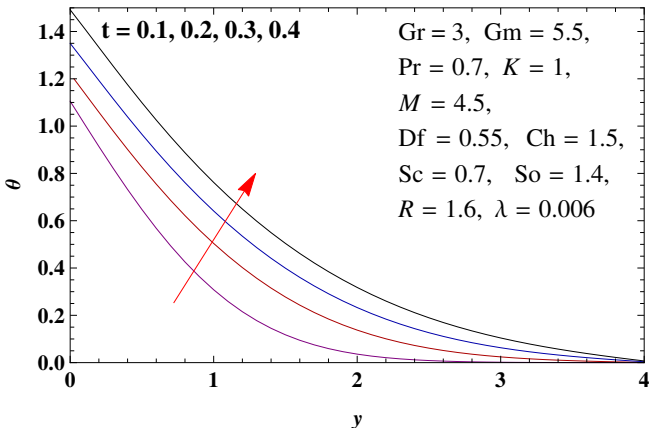

Figure 21. Change in temperature for different values of t

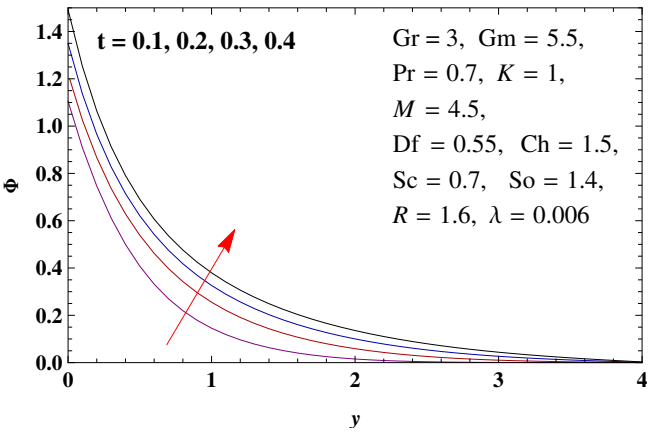

Figure 22. Change in concentration for various values of t

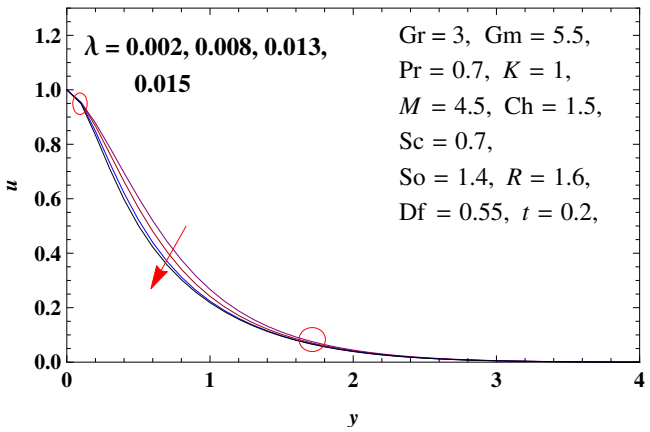

Figure 23. Change in velocity for multiple values of λ

Df	Ch	M	Pr	So	Sc	R	λ	t	τ	Nu	Sh
0.12	1.5	4.5	0.7	1.4	0.7	1.6	0.006	0.2	−0.472645	0.948392	1.87638
0.55	1.5	4.5	0.7	1.4	0.7	1.6	0.006	0.2	−0.465699	0.812433	1.96066
0.98	1.5	4.5	0.7	1.4	0.7	1.6	0.006	0.2	−0.459046	0.658411	2.05901
1.7	1.5	4.5	0.7	1.4	0.7	1.6	0.006	0.2	−0.448964	0.344671	2.2681
0.55	1.2	4.5	0.7	1.4	0.7	1.6	0.006	0.2	−0.451703	0.820627	1.88569
0.55	3.7	4.5	0.7	1.4	0.7	1.6	0.006	0.2	−0.553813	0.761198	2.425
0.55	7.3	4.5	0.7	1.4	0.7	1.6	0.006	0.2	−0.660341	0.699495	2.97482
0.55	12	4.5	0.7	1.4	0.7	1.6	0.006	0.2	−0.759181	0.641605	3.48276
0.55	1.5	0.9	0.7	1.4	0.7	1.6	0.006	0.2	0.557764	0.812433	1.96066
0.55	1.5	2.8	0.7	1.4	0.7	1.6	0.006	0.2	−0.0176971	0.812433	1.96066
0.55	1.5	5.9	0.7	1.4	0.7	1.6	0.006	0.2	−0.795196	0.812433	1.96066
0.55	1.5	7.6	0.7	1.4	0.7	1.6	0.006	0.2	−1.15489	0.812433	1.96066
0.55	1.5	4.5	0.7	1.4	0.7	1.6	0.006	0.2	−0.465699	0.812433	1.96066
0.55	1.5	4.5	2.2	1.4	0.7	1.6	0.006	0.2	−0.520942	1.5645	1.53227
0.55	1.5	4.5	3.6	1.4	0.7	1.6	0.006	0.2	−0.526067	2.33263	0.976689
0.55	1.5	4.5	5.4	1.4	0.7	1.6	0.006	0.2	−0.50555	4.14135	−0.528152
0.55	1.5	4.5	0.7	0.4	0.7	1.6	0.006	0.2	−0.566658	0.79701	2.11244
0.55	1.5	4.5	0.7	3	0.7	1.6	0.006	0.2	−0.297485	0.839804	1.69882
0.55	1.5	4.5	0.7	6.5	0.7	1.6	0.006	0.2	0.113694	0.919725	0.973769
0.55	1.5	4.5	0.7	8.5	0.7	1.6	0.006	0.2	0.39519	0.993497	0.335608
0.55	1.5	4.5	0.7	1.4	0.13	1.6	0.006	0.2	0.0341287	0.930733	0.840377
0.55	1.5	4.5	0.7	1.4	1.4	1.6	0.006	0.2	−0.710647	0.706743	2.88324
0.55	1.5	4.5	0.7	1.4	2.5	1.6	0.006	0.2	−0.931816	0.556285	4.16516
0.55	1.5	4.5	0.7	1.4	3.7	1.6	0.006	0.2	−1.09395	0.385062	5.60749
0.55	1.5	4.5	0.7	1.4	0.7	0.2	0.006	0.2	−0.512985	1.3397	1.67585
0.55	1.5	4.5	0.7	1.4	0.7	2.3	0.006	0.2	−0.449097	0.712088	2.00444
0.55	1.5	4.5	0.7	1.4	0.7	3.6	0.006	0.2	−0.425534	0.597366	2.04952
0.55	1.5	4.5	0.7	1.4	0.7	5	0.006	0.2	−0.406727	0.521646	2.07625
0.55	1.5	4.5	0.7	1.4	0.7	1.6	0.002	0.2	−0.462929	0.812433	1.96066
0.55	1.5	4.5	0.7	1.4	0.7	1.6	0.008	0.2	−0.468193	0.812433	1.96066
0.55	1.5	4.5	0.7	1.4	0.7	1.6	0.013	0.2	−0.48803	0.812433	1.96066
0.55	1.5	4.5	0.7	1.4	0.7	1.6	0.015	0.2	−0.514796	0.812433	1.96066
0.55	1.5	4.5	0.7	1.4	0.7	1.6	0.006	0.1	−1.54572	0.961755	1.96307
0.55	1.5	4.5	0.7	1.4	0.7	1.6	0.006	0.2	−0.465699	0.812433	1.96066
0.55	1.5	4.5	0.7	1.4	0.7	1.6	0.006	0.3	0.209867	0.7808	2.13892
0.55	1.5	4.5	0.7	1.4	0.7	1.6	0.006	0.4	0.76124	0.788366	2.39323

Table 1. Skin friction coefficient S_f, Nusselt number N_Θ and Sherwood number S_Φ for multiple values of parameters taking fix values of $K = 1.4, Gr = 3, Gm = 5.5$

References

[1] M. R. Heydari and A. S. Taleghani, *Analysis of boundary layer in MHD flow of non-Newtonian visco-elastic fluid on stretching sheet*, Bulletin de la Société Royale des Sciences de Liège, 85(2016), 21-33.

[2] Adamu Gizachew and Bandari Shankar, *MHD Flow of Non-Newtonian Viscoelastic Fluid on Stretching Sheet With The Effect of Slip Velocity*, International Journal of Engineering and Manufacturing Science, 8(1)(2018), 1-14.

[3] F. Hussain, F. Mabood, A. Zeeshan and R. Ellahi, *Numerical study on bi-phase coupled stress fluid in the presence of Hafnium and metallic nanoparticles over an inclined plane*, Int. J. Numer. Meth. Heat Fluid Flow, 29(8)(2019), 2854–2869.

[4] G. S. Reddy, A. J. Chamkha and V. Krishna, *Hall effects on unsteady MHD oscillatory free convective flow of second grade fluid through porous medium between two vertical plates*, AIP Phys Fluids, 30(2)(2018), 15–30.

[5] M. E. Hoseini, S. Gholinia and M. Gholinia, *A numerical investigation of free convection MHD flow of Walter's-B nanofluid over an inclined stretching sheet under the impact of Joule heating*, Thermal Sci. Eng. Progress, 11(2019), 272–282.

[6] T. G. Rao, K. V. B. Rajakumar, M. U. Reddy and K. S. Balamurugan, *Influence of Dufour and thermal radiation on unsteady MHD Walter's liquid model-B flow past an impulsively started infinite vertical plate embedded in a porous medium with chemical reaction, Hall and ion slip current*, SN Appl. Sci., 2(2020), 742.

[7] M. Idrees, Z. Shah, A. Dawar, A. Saeed, S. Islam and W. Khan, *Entropy generation in MHD flow of carbon nanotubes in a rotating channel with four different types of molecular liquids*, Int. J. Heat Technol., 37(2019), 509–519.

[8] Sewli Chatterijee, Dulal Pal H. Mondal and Sibanda Precious, *Thermophoresis and soret-dufour on MHD mixed convection mass transfer over an inclined plate with non-uniform heat source/sink and chemical reaction*, Ain Shams Eng. J., 9(4(2018), 2111–2121.

[9] Rahila Naz, Sana Tariq and Hamed Alsulami, *Inquiry of entropy generation in stratified Walters' B nanofluid with swimming gyrotactic microorganisms*, Alexandria Engineering Journal, 59(2020), 247–261.

[10] R. M. Akram, K. Jabeen and M. Mushtaq, *A comparative study of MHD flow analysis in a porous medium by using differential transformation method and variational iteration method*, Journal of Contemporary Applied Mathematics, 9(2)(2019), 1–15.

[11] K. Jabeen, M. Mushtaq, and R. M. Akram, *Analysis of the MHD boundary layer flow over a nonlinear stretching sheet in a porous medium using semianalytical approaches*, Hindawi Mathematical Problems in Engineering, 2020(2020), Article ID 3012854.

[12] A. S. Idowu, B. O. Falodun, *Variable thermal conductivity and viscosity effects on non-Newtonian fluids flow through a vertical porous plate under Soret-Dufour influence*, Mathematics and Computers in Simulation, 177(2020), 358–384.

[13] H. A. Luther, B. Carnahan and J. O. Wilkes, *Applied Numerical Methods*, Krieger Pub Co, Florida, (1990).

[14] J. R. Howell and R. Siegel, *Thermal Radiation Heat Transfer*, Taylor & Francis, London, (1992).